

The LBNO long-baseline oscillation sensitivities with two conventional neutrino beams at different baselines

S.K. Agarwalla,^o L. Agostino,^a M. Aittola,^u A. Alekou,^b B. Andrieu,^x F. Antoniou,^b
R. Asfandiyarov,^{aa} D. Autiero,^y O. Bésida,^k A. Balik,^r P. Ballett,ⁿ I. Bandac,^k
D. Banerjee,^g W. Bartmann,^b F. Bay,^g B. Biskup,^b A.M. Blebea-Apostu,ⁱ A. Blondel,^{aa}
M. Bogomilov,^c S. Bolognesi,^k E. Borriello,^{ab} I. Brancus,ⁱ A. Bravar,^{aa}
M. Buizza-Avanzini,^a D. Caiulo,^y M. Calin,^z M. Calviani,^b M. Campanelli,^d C. Cantini,^g
G. Cata-Danil,ⁱ S. Chakraborty,^{ab} N. Charitonidis,^b L. Chaussard,^y D. Chesneau,ⁱ
F. Chipiesiu,ⁱ P. Crivelli,^g J. Dawson,^a I. De Bonis,^r Y. Declais,^y P. Del Amo Sanchez,^r
A. Delbart,^k S. Di Luise,^g D. Duchesneau,^r J. Dumarchez,^x I. Efthymiopoulos,^b
A. Eliseev,^w S. Emery,^k T. Enqvist,^u K. Enqvist,^e L. Epprecht,^g A.N. Erykalov,^w
T. Esanu,^z D. Franco,^y M. Friend,^h V. Galymov,^y G. Gavrilov,^w A. Gendotti,^g
C. Giganti,^x S. Gilardoni,^b B. Goddard,^b C.M. Gomoiu,^{z,i} Y.A. Gornushkin,^q
P. Gorodetzky,^a A. Haesler,^{aa} T. Hasegawa,^h S. Horikawa,^g K. Huitu,^e A. Izmaylov,^m
A. Jipa,^z K. Kainulainen,^f Y. Karadzhev,^{aa} M. Khabibullin,^m A. Khotjantsev,^m
A.N. Kopylov,^m A. Korzenev,^{aa} S. Kosyanenko,^w D. Kryn,^a Y. Kudenko,^{m,t,s}
P. Kuusiniemi,^u I. Lazanu,^z C. Lazaridis,^b J.-M. Levy,^x K. Loo,^f J. Maalampi,^f
R.M. Margineanu,ⁱ J. Marteau,^y C. Martin-Mari,^{aa} V. Matveev,^{m,q} E. Mazzucato,^k
A. Mefodiev,^m O. Mineev,^m A. Mirizzi,^{ab} B. Mitrica,ⁱ S. Murphy,^g T. Nakadaira,^h
S. Narita,^p D.A. Nesterenko,^w K. Nguyen,^g K. Nikolics,^g E. Noah,^{aa} Yu. Novikov,^w
A. Oprima,ⁱ J. Osborne,^b T. Ovsyannikova,^m Y. Papaphilippou,^b S. Pascoli,ⁿ
T. Patzak,^{a,l} M. Pectu,ⁱ E. Pennacchio,^y L. Periale,^g H. Pessard,^r B. Popov,^x
M. Ravonel,^{aa} M. Rayner,^{aa} F. Resnati,^g O. Ristea,^z A. Robert,^x A. Rubbia,^g
K. Rummukainen,^e A. Saftoiu,ⁱ K. Sakashita,^h F. Sanchez-Galan,^b J. Sarkamo,^u
N. Saviano,^{ab,n} E. Scantamburlo,^{aa} F. Sergiampietri,^{g,j} D. Sgalaberna,^g
E. Shaposhnikova,^b M. Slupecki,^f D. Smargianaki,^b D. Stanca,ⁱ R. Steerenberg,^b
A.R. Sterian,ⁱ P. Sterian,ⁱ S. Stoica,ⁱ C. Strabel,^b J. Suhonen,^f V. Suvorov,^w G. Toma,ⁱ
A. Tonazzo,^a W.H. Trzaska,^f R. Tsenov,^c K. Tuominen,^e M. Valram,ⁱ
G. Vankova-Kirilova,^c F. Vannucci,^a G. Vasseur,^k F. Velotti,^b P. Velten,^b V. Venturi,^b
T. Viant,^g S. Vihonen,^f H. Vincke,^b A. Vorobyev,^w A. Weber,^v S. Wu,^g N. Yershov,^m
L. Zambelli,^h M. Zito^k

^aAPC, AstroParticule et Cosmologie, Université Paris Diderot, CNRS/IN2P3, CEA/Irfu, Observatoire de Paris, Sorbonne Paris Cité, 10, rue Alice Domon et Léonie Duquet, 75205 Paris Cedex 13, France

^bCERN, Geneva, Switzerland

¹Now at Instituut voor Kern- en Stralingsfysica, KU Leuven, 3001 Leuven, Belgium.

- ^cDepartment of Atomic Physics, Faculty of Physics, St. Kliment Ohridski University of Sofia, Sofia, Bulgaria
- ^dDepartment of Physics and Astronomy, University College London, London, United Kingdom
- ^eDepartment of Physics, University of Helsinki, Helsinki, Finland
- ^fDepartment of Physics, University of Jyväskylä, Jyväskylä, Finland
- ^gETH Zurich, Institute for Particle Physics, Zurich, Switzerland
- ^hHigh Energy Accelerator Research Organization (KEK), Tsukuba, Ibaraki, Japan
- ⁱHoria Hulubei National Institute of R&D for Physics and Nuclear Engineering, IFIN-HH, Romania
- ^jINFN-Sezione di Pisa, Pisa, Italy
- ^kIRFU, CEA Saclay, Gif-sur-Yvette, France
- ^lInstitut Universitaire de France, Maison des Universités, 103, boulevard Saint-Michel 75005 Paris, France
- ^mInstitute for Nuclear Research of the Russian Academy of Sciences, Moscow, Russia
- ⁿInstitute for Particle Physics Phenomenology, Department of Physics, Durham University, United Kingdom
- ^oInstitute of Physics, Sachivalaya Marg, Sainik School Post, Bhubaneswar 751005, India
- ^pIwate University, Department of Electrical Engineering and Computer Science, Morioka, Iwate, Japan
- ^qJoint Institute for Nuclear Research, Dubna, Moscow Region, Russia
- ^rLAPP, Université de Savoie, CNRS/IN2P3, F-74941 Annecy-le-Vieux, France
- ^sMoscow Institute of Physics and Technology, Moscow region, Russia
- ^tNational Research Nuclear University "MEPhI", Moscow, Russia
- ^uOulu Southern Institute and Department of Physics, University of Oulu, Finland
- ^vOxford University, Department of Physics, Oxford, United Kingdom
- ^wPetersburg Nuclear Physics Institute (PNPI), St-Petersburg, Russia
- ^xUPMC, Université Paris Diderot, CNRS/IN2P3, Laboratoire de Physique Nucléaire et de Hautes Energies (LPNHE), Paris, France
- ^yUniversité de Lyon, Université Claude Bernard Lyon 1, IPN Lyon (IN2P3), Villeurbanne, France
- ^zUniversity of Bucharest, Faculty of Physics, Bucharest-Magurele, Romania
- ^{aa}University of Geneva, Section de Physique, DPNC, Geneva, Switzerland
- ^{ab}University of Hamburg, Hamburg, Germany

ABSTRACT: The proposed Long Baseline Neutrino Observatory (LBNO) initially consists of ~ 20 kton liquid double phase TPC complemented by a magnetised iron calorimeter, to be installed at the Pyhäsalmi mine, at a distance of 2300 km from CERN. The conventional neutrino beam is produced by 400 GeV protons accelerated at the SPS accelerator delivering 700 kW of power. The long baseline provides a unique opportunity to study neutrino flavour oscillations over their 1st and 2nd oscillation maxima exploring the L/E behaviour, and distinguishing effects arising from δ_{CP} and matter. In this paper we show how this comprehensive physics case can be further enhanced and complemented if a neutrino beam produced at the Protvino IHEP accelerator complex, at a distance of 1160 km, and with modest power of 450 kW is aimed towards the same far detectors. We show that the coupling of two independent sub-MW conventional neutrino and antineutrino beams at different baselines from CERN and Protvino will allow to measure CP violation in the leptonic sector at a confidence level of at least 3σ for 50% of the true values of δ_{CP} with a 20 kton detector. With a far detector of 70 kton, the combination allows a 3σ sensitivity for 75% of the true values of δ_{CP} after 10 years of running. Running two independent neutrino beams, each at a power below 1 MW, is more within today's state of the art than the long-term operation of a new single high-energy multi-MW facility, which has several technical challenges and will likely require a learning curve.

Contents

1	Introduction	1
2	Choice of the baseline distance	2
2.1	CP violation sensitivity	3
2.2	Mass hierarchy determination sensitivity	4
2.3	Benefits of the dual baseline configuration	5
3	Experimental setup	6
3.1	The Protvino accelerator complex	6
3.2	Simulation of the neutrino beamlines	6
4	CP violation determination in the dual baseline configuration	8
4.1	Experimental observables	9
4.2	Fit and analysis method	9
5	Results	13
5.1	CP-violation discovery potential for the dual beam facility	14
5.2	Advantages of the dual baseline configuration	14
6	Conclusions	16

1 Introduction

Neutrino masses and oscillations are, to this day, the only experimentally established evidence of physics Beyond the Standard Model (BSM). In the three neutrino framework the oscillations of massive neutrinos are described via the Pontecorvo-Maki-Nakagawa-Sakata (PMNS [1, 2]) matrix. This 3×3 unitary matrix U is generally parameterized in terms of the three mixing angles θ_{12} , θ_{13} , θ_{23} , and the CP violating Dirac phase δ_{CP} (neglecting Majorana phases). The parameter δ_{CP} is the phase that controls the CP asymmetry.

In addition to the known θ_{12} and θ_{23} , the recent measurement of the last mixing angle θ_{13} [3, 4], opened the way to a new generation of long-baseline neutrino oscillation experiments. The major goals of future long-baseline experiments such as the proposed LBNO [5, 6], LBNE [7, 8] and HyperKamiokande [9] are the conclusive determination of the mass hierarchy (MH) and the search for leptonic CP-violation (CPV) via the determination of δ_{CP} .

The strategy of LBNO is the outcome of the extensive feasibility studies LAGUNA and LAGUNA-LBNO which lasted 6 years [10, 11]. LBNO aims at the construction of a double phase liquid argon neutrino observatory [12] complemented by a magnetised muon detector (MIND) [13], located deep-underground at the Pyhäsalmi mine. The long-baseline

neutrino oscillation programme uses a wide-band beam from the CERN SPS accelerator at a distance of 2300 km.

In LBNO with a baseline of 2300 km, the L/E dependence of the $\nu_\mu \rightarrow \nu_e$ and of the $\bar{\nu}_\mu \rightarrow \bar{\nu}_e$ oscillation probabilities and the very long neutrino path through Earth allow to address both fundamental questions, the ordering of neutrino mass eigenstates and CP violation in the lepton sector, in clean experimental conditions. This can be achieved by profiting from the ability to reverse the focusing horns polarity and from the well controlled fluxes typical of neutrino produced by accelerators. Its physics potential has been extensively evaluated previously [5, 6, 14].

It was shown that a few years of running with the CERN SPS at 700 kW beam power and a 20 kton far detector mass provides a direct and guaranteed discovery of MH ($> 5\sigma$) over the full phase space of oscillation parameters, and a significance for CPV above 3σ for $\sim 25(40)\%$ of the δ_{CP} values under the expectation that $\sin^2 2\theta_{13}$ will be known with a precision of $\pm 10(2.5)\%$. The setup with a 2300 km baseline allows to optimise the conventional neutrino flux to a broad band beam covering both 1st and 2nd maximum optimising the sensitivity for CPV and is less sensitive to the assumed systematic errors, compared to the LBNE and HyperKamiokande setups [6].

In this paper, we present the physics potential of LBNO if the setup were further coupled to an additional neutrino beam from the Protvino IHEP facility at a distance of 1160 km (See Fig. 1). There, an existing proton synchrotron accelerator up to 70 GeV could be upgraded to reach a modest beam power of 400-450 kW and produce a neutrino beam aimed to the Pyhäsalmi mine. We show that the physics case for a long baseline neutrino beam can be strengthened by a dual beam setup. There is a great experience worldwide, especially at the CERN SPS, in running conventional neutrino beams with powers ranging from 200-400 kW. Within the next decade, the NuMI beam at FNAL is planned to operate up to 700 kW [15]. Running two independent neutrino beams, each at a power below 1 MW, is more practical and within known domains of experience than the long-term operation of a new single high-energy multi-MW facility, which has several technical challenges and will likely require a learning curve. Therefore the approach discussed in this paper with two sub-MW conventional neutrino beams would have several technical advantages and rely on existing and proven neutrino beam technologies.

The structure of this paper is as follows. In Section 2 we review how the baseline choice influences the physics reach of a long-baseline experiment and which advantages a dual beam facility offers. In Section 3, we introduce the Protvino facility and discuss the beam specifications at this site. We present the details of our simulations and analyses in Section 4, and our results will be shown in Section 5.

2 Choice of the baseline distance

A main parameter in a long-baseline experiment is the choice of the baseline. The distance between the source of the neutrinos and the detector influences the physics potential of the facility in a number of ways. In the setup considered in this paper we studied two



Figure 1. View of the dual beamline configuration: CERN to Pyhäsalmi (2300 km) and Protvino to Pyhäsalmi (1160 km).

independent and different baselines: (1) the CERN to Pyhäsalmi beam (C2P) with 2300 km and (2) the Protvino to Pyhäsalmi beam (P2P) with 1160 km.

2.1 CP violation sensitivity

A well known property of the neutrino oscillation phenomenon is that the CP asymmetry increases from the first to higher orders oscillation maxima (see e.g. [16]). This is understood by the fact that asymmetry due to CP has an envelope determined by [17]:

$$\frac{2s_{\delta}c_{12}s_{12}}{s_{13}} \cot \theta_{23} \frac{\Delta m_{21}^2 L}{2E} \quad (2.1)$$

which grows as a function of L/E . The 2nd maximum (the one at lower energy) is hence more sensitive to CPV than the 1st maximum and an experiment able to access the information from the 2nd maximum will have a better sensitivity to δ_{CP} .

The oscillation probability for P2P and C2P are shown in Fig. 2. In the plots, the probabilities have a Gaussian smearing applied to the neutrino energy in order to illustrate the effects of detector resolution. Looking at the probabilities, one can infer that spectral regions of interest are around the 1st and the 2nd maximum, and the regions in-between. For P2P the second maximum region appears at rather low energies of about 0.5-1 GeV. For C2P due to its longer baseline, the second maximum occurs between 1-2 GeV. The technical limitations of conventional neutrino beams are well understood and with current technological limits on magnetic field strengths and volumes, they are not efficient at focusing hadrons with energies below ~ 1 GeV [8]. Access to the 2nd oscillation maximum is therefore more easily achieved with longer baselines. Taking into account vanishing neutrino cross-sections at low energies (in particular for antineutrinos), the measurement

of the 2nd oscillation maximum requires in practice a baseline greater than 1500 km [6]. The $\nu_\mu \rightarrow \nu_\tau$ CC events where $\tau \rightarrow e\nu\nu$, which become more important at longer baselines due to the higher energy tails of the neutrino flux, act a priori as a background to electron appearance. But, as shown in Refs. [5, 6], they can be kinematically separated exploiting the excellent kinematic reconstruction of liquid argon detectors. In conclusion, the longer baseline C2P option is more favorable for the observation of events in the second maximum, but both P2P and C2P populate efficiently the region of the first maximum.

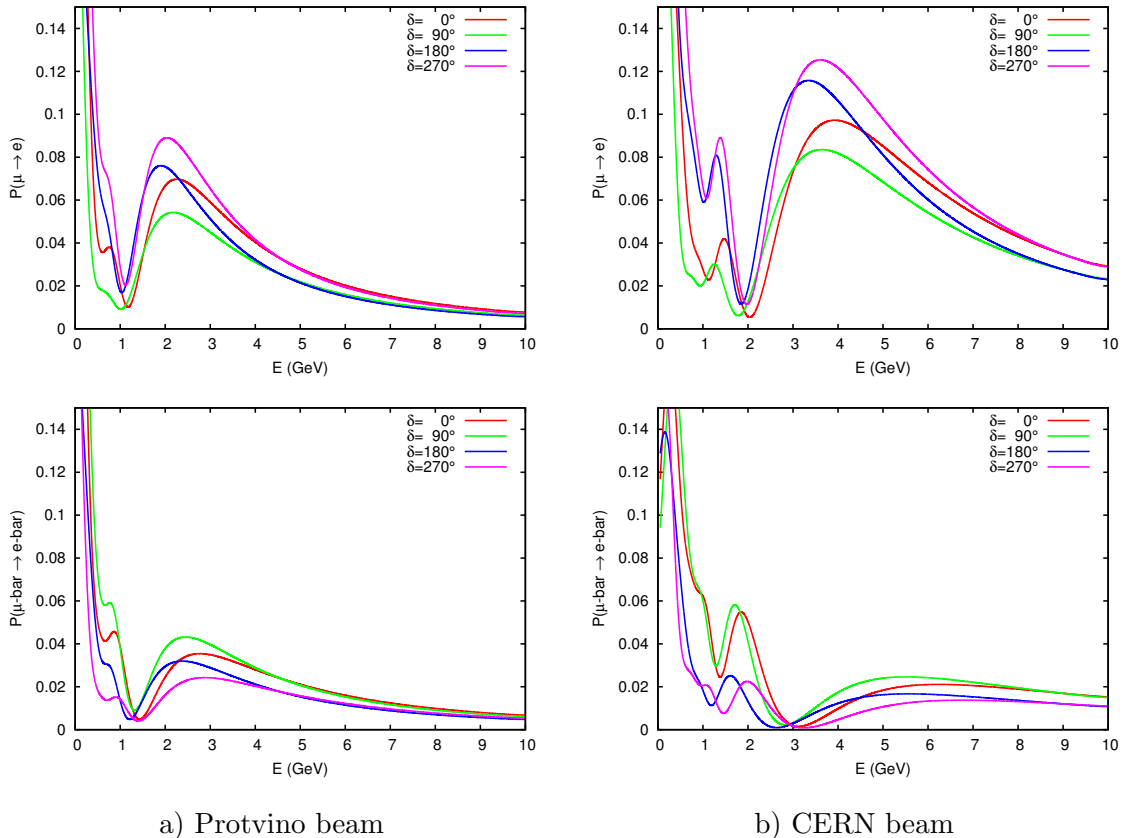


Figure 2. Top row (bottom row): the ν_μ to ν_e ($\bar{\nu}_\mu$ to $\bar{\nu}_e$) oscillation probability at the Pyhäsalmi site for a selection of true values of δ_{CP} . These plots assume normal mass ordering and have a Gaussian smear applied, as discussed in the text.

2.2 Mass hierarchy determination sensitivity

For sufficiently long baselines, the mass hierarchy can be determined thanks to the effect on the oscillation probabilities of the passage through the Earth. Matter effects modify the propagation, with an enhancement of the ν_e appearance probability for the neutrinos and a suppression for the antineutrinos for a normal hierarchy. If the mass ordering is inverted, the opposite happens. By comparing the oscillation probabilities for neutrinos and antineutrinos, it is possible to deduce MH. The magnitude of this effect increases as a

function of baseline distance, which can be seen in Fig. 3. The longer baseline from CERN to Pyhäsalmi leads to a more pronounced separation for the two mass orderings, especially around the first oscillation maximum. In the following we will not show the impact of adding P2P to determine the mass hierarchy since this will be determined in few years of running by C2P alone [14].

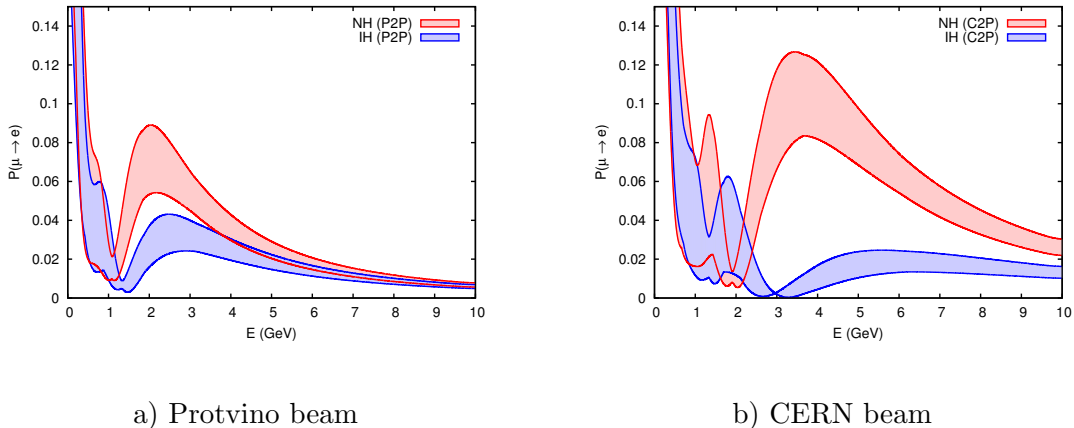


Figure 3. ν_μ to ν_e oscillation probability at the Pyhäsalmi site for two possible mass orderings: normal (NH) and inverted (IH) hierarchy. The width of each band shows the variation in probability induced by the parameter δ_{CP} .

2.3 Benefits of the dual baseline configuration

It is known since a long time that the inference of the oscillation parameters in long-baseline experiments is complicated by the problem of degeneracies [18]. In vacuum three such degeneracies can be identified: *i*) the intrinsic degeneracy under which θ_{13} and δ_{CP} have clone values; *ii*) the sign degeneracy, as in vacuum it is possible to change the sign of Δm_{31}^2 and δ_{CP} to $\pi - \delta_{CP}$ without affecting the probabilities. This degeneracy is broken by matter effects. Sufficiently long baselines, for which matter effects are more significant, are therefore preferred; *iii*) the octant of θ_{23} , if this angle is not maximal. At present, the octant is not known.

The known problem of the degeneracies can be mitigated by having access to a wide band oscillation spectrum, where the information at different energies acts in a complementary fashion to resolve any ambiguities. We have studied and reported the optimisation of such a wide-band beam elsewhere[14]. This strategy is advanced further with the combination of P2P and C2P, where information is collected from two broad spectra focused on overlapping yet different parts of the L/E spectrum.

3 Experimental setup

3.1 The Protvino accelerator complex

The IHEP accelerator complex consists of four accelerators connected in a cascade as shown in Fig. 4. A 30 MeV linear accelerator serves as an injector for a 1.5 GeV rapid cycling booster synchrotron, a 100 MeV Alvarez type linear accelerator which serves as a light-ion or a back-up proton injector feeding the 1.5 GeV synchrotron, and a 70 GeV proton synchrotron which now operates at 50 GeV with a beam power of 8-15 kW. The experimental program includes studies of rare kaon decays, hadron spectroscopy, spin physics and hadron-nuclei interactions. A dedicated neutrino beam line has also been constructed and used for several experiments at U-70, e.g. the IHEP-JINR Neutrino Detector [19]. An upgrade of a beam power to 400-450 kW is envisioned in the future as an extension of the Omega Project [20]. We assume in the following that this power is available for a new neutrino beam line directed towards Pyhäsalmi.

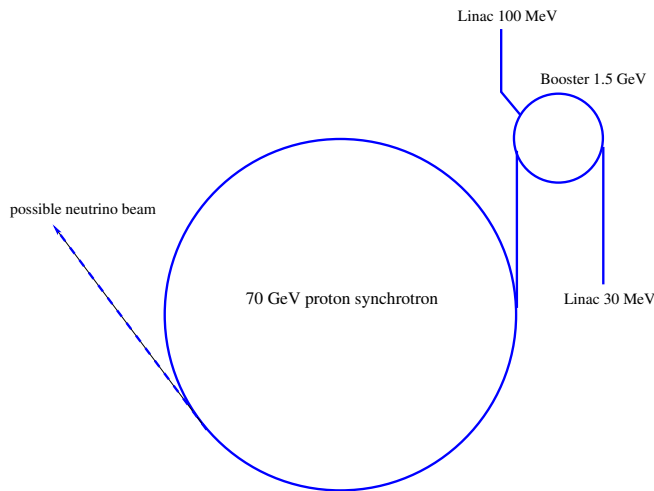


Figure 4. Schematic view of the IHEP accelerator complex.

3.2 Simulation of the neutrino beamlines

For this study, we assume a proton beam energy of 70 GeV and a power of 450 kW on the neutrino target. The neutrino beam simulation for the Protvino site is based on the simulation code developed in the context of the first phase LAGUNA design study [21]. The hadron production target is modeled as a cylinder, which is 4 mm in diameter and 1 m long and is made from light density ($\rho = 1.85 \text{ g/cm}^3$) graphite. The focusing system consists of two horns with parabolic inner conductors. The shape of the inner conductors as well as the distance between the horns are taken to be the same as in [5]. A two-dimensional layout of the horn-target system is shown in Fig. 5.

To optimize the energy spectrum of the neutrino beam we varied the longitudinal position of the target and the currents in the horns. The values of these parameters

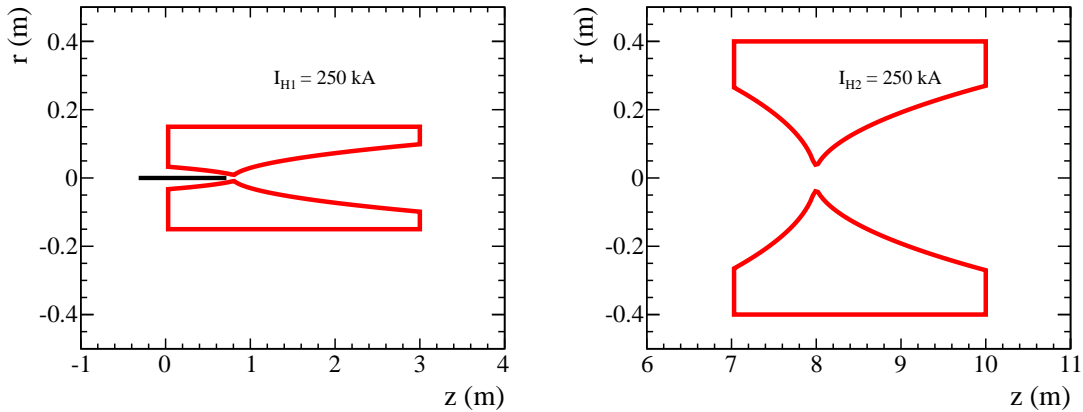


Figure 5. Illustration of the target and horn geometry.

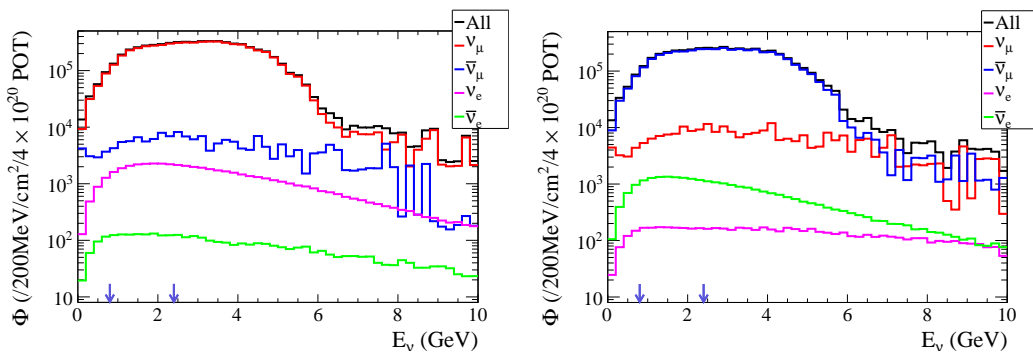


Figure 6. Neutrino (left) and antineutrino (right) fluxes for Protvino-to-Pyhäsalmi (P2P). The arrows indicate the energy of the first (arrow on the right) and second (arrow on the left) oscillation maxima.

were randomly drawn from uniform distributions with realistic limits. The merit of each configuration was then evaluated based on a sensitivity to CPV. The optimal value for the target position was found to be -0.3 m upstream of the first horn, while the optimal horn current was determined to be 250 kA [5]. The radius and the length of the decay tunnel were fixed to 1.5 m and 400 m, respectively.

The composition of the non-oscillated fluxes for the P2P and C2P baselines are shown in Fig. 6 and Fig. 7. These fluxes are normalized to 4×10^{20} protons on target. With a 450 kW operation this number corresponds to about one year of accelerator running with fast extraction, where a year is assumed to correspond to 10^7 s. For the simulation of C2P, we have followed the new optimisation of the SPS fluxes described in [14]. The so-called GLB optimisation has been used as default and the low energy option has been used for cross-check. A summary of the proton beam parameters used in this paper for C2P and P2P are shown in Tab. 1

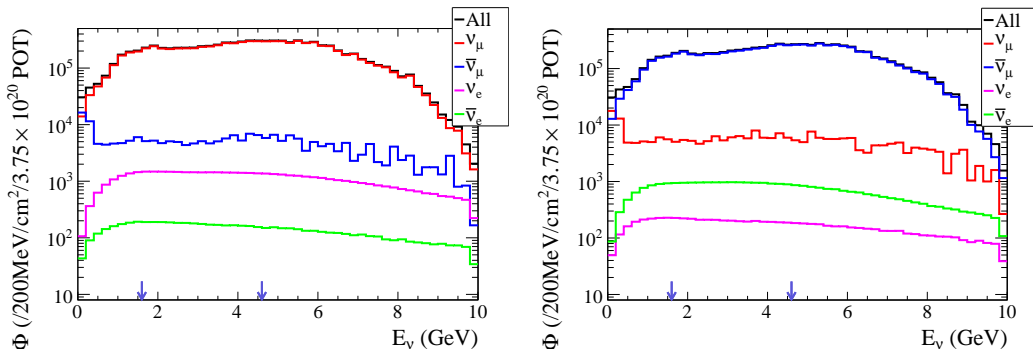


Figure 7. Neutrino (left) and antineutrino (right) fluxes for CERN-to-Pyhäsalmi (C2P). The arrows indicate the energy of the first (arrow on the right) and second (arrow on the left) oscillation maxima.

Table 1. Assumed parameters of the primary protons for the C2P and the P2P beams.

Parameter	C2P beam	P2P beam
E_{beam} (GeV)	400	70
I_{beam} (ppp)	7×10^{13}	2.2×10^{14}
Cycle length (s)	6	5
P_{beam} (kW)	750	450
POT_{year} (10^{20})	$1.0 \div 1.4$	4

4 CP violation determination in the dual baseline configuration

In this section we focus on the benefit of the dual baseline configuration for the discovery of CP violation in the leptonic sector. We do not show results for the determination of the MH since the C2P setup alone already provide a guaranteed measurement ($> 5\sigma$) of the mass hierarchy within few years [5, 6, 14].

In order to compare setups, we have performed simulations of the P2P and C2P cases both individually and in combination. The primary channel of interest is the appearance channel, $\nu_{\mu} \rightarrow \nu_e$ ($\bar{\nu}_{\mu} \rightarrow \bar{\nu}_e$), as it is particularly sensitive to $\text{sign}(\Delta m_{31}^2)$ and δ_{CP} . We have also included the disappearance channel as it plays an important role in the precise determination of the value of Δm_{31}^2 and θ_{23} , and indirectly on the precision with which one can determine δ_{CP} . The true value of θ_{23} has a significant influence on the sensitivity to δ_{CP} [6]. The solar parameters (Δm_{31}^2 and θ_{13}) are fixed in the fit since their impact on the results is negligible.

We consider the following background contributions to the signal e-like events:

- Intrinsic ν_e contamination in the beam (intrinsic ν_e),
- Electron events from ν_{τ} charged current interaction with subsequent leptonic τ decay ($\nu_{\tau} \rightarrow e$ contamination),
- Neutral current ν_{μ} events with π^0 production (NC π^0),

- Mis-identified muons from ν_μ CC interactions (mis-id ν_μ).

A detailed description of neutrino event simulations and selection efficiency can be found in [5].

4.1 Experimental observables

As experimental observables we use reconstructed neutrino energy, E_ν^{rec} , and missing momentum in the transverse plane, defined by the incoming neutrino beam direction, p_T^{miss} , of each e-like event to construct bi-dimensional distributions used to discriminate signal from background. Examples of such distributions are shown in Fig. 8 for a value of $\delta_{CP} = 0$ and the case of normal mass hierarchy for the P2P case. As can be seen in the figure, the shape of the signal and background contributions in the $E_\nu^{\text{rec}} - p_T^{\text{miss}}$ phase-space differ. In particular, NC π^0 interactions are characterized by low E_ν^{rec} values, while events originating from ν_τ CC interactions tend to have larger p_T^{miss} than the ν_e CC events because of the two neutrinos in the final state. This allows a better signal-background discrimination than if one were to use E_ν^{rec} information only. In the case of the μ -like events only the reconstructed neutrino energy is used since the background components in this sample are smaller.

4.2 Fit and analysis method

The key ingredient to be provided to the fit are the priors for the oscillation parameters \mathbf{o} and for the detector systematic uncertainties \mathbf{f} . For both sets of uncertainties we have used the same parameters described for the LBNO CPV reach using CERN beams. The assumed values of the oscillation parameters \mathbf{o} are given in Tab. 2. The parameters whose values are not labeled as “exact” are allowed to vary in the fit.

Parameter	Central value	Uncertainty
Δm_{21}^2	$7.45 \times 10^{-5} \text{ eV}^2$	exact
$ \Delta m_{32}^2 $	$2.5 \times 10^{-3} \text{ eV}^2$	3.75%
$\sin^2 \theta_{12}$	0.31	exact
$\sin^2 2\theta_{13}$	0.09	3%
$\sin^2 \theta_{23}$	0.45	5%

Table 2. Assumed values of the oscillation parameters.

Tab. 3 summarizes the assumptions on the Earth density and systematic uncertainties on the expected number of events for the different components contributing to the electron-like sample. Due to the difference in the baselines, the average matter density encountered by each neutrino beam may not be the same. The Earth density for C2P have been extensively studied in the context of LAGUNA-LBNO and it was found to be 3.2 g/cm^3 . For the Protvino beam we have checked that the CPV sensitivity does not depend on the Earth density if this parameter is varied between 3.2 and 2.8 g/cm^3 . In the combination the value of the Earth density is fixed to 3.2 g/cm^3 for both the baselines.

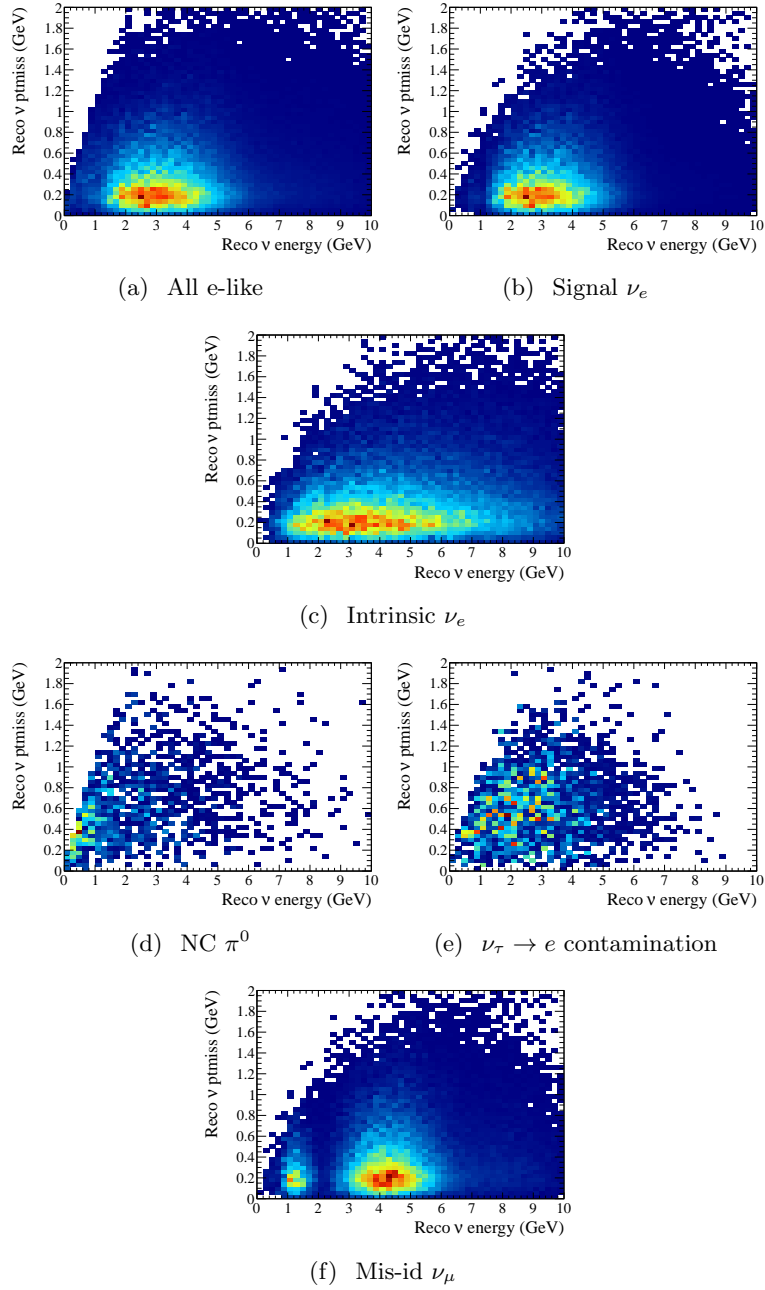


Figure 8. Example event distributions in the $E_\nu^{rec} - p_T^{miss}$ phase-space for various channels contributing to the P2P e-like sample. $\delta_{CP} = 0$ and NH hierarchy are assumed.

In the fit we minimize the following χ^2 with respect to the oscillation and systematic parameters:

$$\chi^2 = \chi_{\text{appear}}^2 + \chi_{\text{disa}}^2 + \chi_{\text{syst}}^2. \quad (4.1)$$

The χ_{appear}^2 is the term corresponding to the electron-like sample. It is given by the sum over the beamline i (C2P or P2P), the horns polarity j (positive or negative) and the

Name	Central value	Uncertainty	Correlation (ρ_i)
Earth density (g/cm ³)	3.2	4%	[0, 1]
Signal event normalization f_{sig}	1.0	3%	[0, 1]
Beam ν_e normalization f_{ν_e}	1.0	5%	[0, 1]
Tau event normalization f_{ν_τ}	1.0	20%	[0, 1]
ν NC and ν_μ CC background f_{NC}	1.0	10%	[0, 1]

Table 3. Assumptions on the matter density and the uncertainties on the event normalizations for two beams. These parameters can be treated as uncorrelated or correlated between the two beams by changing the value of ρ_i .

bin k in the $E_\nu^{\text{rec}} - p_T^{\text{miss}}$ phase-space:

$$\chi_{\text{appear}}^2 = 2 \sum_i \sum_j \sum_k R^{e\text{-like}}(i, j, k), \quad (4.2)$$

For each $E_\nu^{\text{rec}} - p_T^{\text{miss}}$ bin, $R^{e\text{-like}}$ is given by:

$$\begin{aligned} R^{e\text{-like}} = & n_e(E_\nu^{\text{rec}}, p_T^{\text{miss}}; \mathbf{o}_{\text{test}}, \mathbf{f}_{\text{test}}) - n_e(E_\nu^{\text{rec}}, p_T^{\text{miss}}; \mathbf{o}_{\text{true}}, \mathbf{f}_{\text{true}}) \\ & + n_e(E_\nu^{\text{rec}}, p_T^{\text{miss}}; \mathbf{o}_{\text{true}}, \mathbf{f}_{\text{true}}) \ln \frac{n_e(E_\nu^{\text{rec}}, p_T^{\text{miss}}; \mathbf{o}_{\text{true}}, \mathbf{f}_{\text{true}})}{n_e(E_\nu^{\text{rec}}, p_T^{\text{miss}}; \mathbf{o}_{\text{test}}, \mathbf{f}_{\text{test}})}, \end{aligned} \quad (4.3)$$

where the subscript *true* (*test*) refers to the true (*test*) values of the \mathbf{o} and \mathbf{f} parameters. The *true* parameters are those chosen by Nature, while *test* refer to the parameter at which we compute the likelihood with respect to the *true* value. The number of the e-like events in a given $E_\nu^{\text{rec}} - p_T^{\text{miss}}$ bin is determined according to:

$$\begin{aligned} n_e(E_\nu^{\text{rec}}, p_T^{\text{miss}}; \mathbf{o}, \mathbf{f}) = & f_{\text{sig}} n_{e\text{-sig}}(E_\nu^{\text{rec}}, p_T^{\text{miss}}; \mathbf{o}) \\ & + f_{\nu_e} n_{\nu_e}(E_\nu^{\text{rec}}, p_T^{\text{miss}}; \mathbf{o}) + f_{\nu_\tau} n_{e,\nu_\tau}(E_\nu^{\text{rec}}, p_T^{\text{miss}}; \mathbf{o}) \\ & + f_{\text{NC}}(n_{\text{NC}\pi^0}(E_\nu^{\text{rec}}, p_T^{\text{miss}}; \mathbf{o}) + n_{\text{mis-}\nu_\mu}(E_\nu^{\text{rec}}, p_T^{\text{miss}}; \mathbf{o})), \end{aligned} \quad (4.4)$$

where $n_{e\text{-sig}}$, n_{ν_e} , n_{e,ν_τ} , $n_{\text{NC}\pi^0}$, and $n_{\text{mis-}\nu_\mu}$ are the number of events for signal, intrinsic beam ν_e , electrons from tau decay, neutral current and mis-identified ν_μ respectively.

For the disappearance channel, the information is contained in the χ_{disa}^2 term of total χ^2 in Eq. 4.1. Similarly to Eq. 4.2 χ_{disa}^2 is given by:

$$\chi_{\text{disa}}^2 = 2 \sum_i \sum_j \sum_k R^{\mu\text{-like}}. \quad (4.5)$$

where i refer to the baseline, j to the polarity and k to the reconstructed energy bin. $R^{\mu\text{-like}}$ is calculated in the same way as in Eq. 4.3, but using the μ -like event distributions. The number of μ -like events in a given bin is the sum of signal $n_{\mu\text{-sig}}$ and $\tau \rightarrow \mu$ background n_{μ,ν_τ} contributions:

$$n_\mu(E_\nu^{\text{rec}}; \mathbf{o}, \mathbf{f}) = f_{\text{sig}} n_{\mu\text{-sig}}(E_\nu^{\text{rec}}; \mathbf{o}) + f_{\nu_\tau} n_{\mu,\nu_\tau}(E_\nu^{\text{rec}}; \mathbf{o}). \quad (4.6)$$

The prior constraints of the oscillation parameters and the systematics are contained in χ_{syst}^2 that has a different form for correlated and uncorrelated terms.

When performing the fit of the dual beam experiment it is important to properly take into account these potential correlations. In our analysis the oscillation parameters are always treated as fully correlated between the two neutrino beams, whilst the normalization parameters listed in Tab. 3 can be treated with varying degree of correlation. This is done by introducing two nuisance parameters and a correlation coefficient (ρ_i) for each systematic uncertainty listed in Tab. 3. For example, to treat the normalization uncertainty on the signal we introduce the nuisance parameters $f_{\text{sig}}^{\text{C2P}}$ and $f_{\text{sig}}^{\text{P2P}}$ for each ν beam and a correlation coefficient $\rho_{f_{\text{sig}}}$. These two parameters would be varied independently in the fit if $\rho_{f_{\text{sig}}} = 0$ or with a degree of correlation fixed by the choice of $\rho_{f_{\text{sig}}} > 0$.

The oscillation and the systematic parameters which are fully correlated between the two beams are constrained through the $\chi_{i,\text{syst}}^2$ term which has the form

$$\chi_{i,\text{syst}}^2 = \frac{(a_i - a_{0,i})^2}{\sigma_{a_i}^2}, \quad (4.7)$$

where $a_{0,i}$ (a_i) is the prior (test) value of the i^{th} parameter and σ_{a_i} is the corresponding prior uncertainty.

In the case when the i^{th} source of systematic uncertainty is parametrized with two nuisance parameters $a_{i,1}$ and $a_{i,2}$ and some correlation coefficient ρ_i (e.g., signal normalization), the constraint term has the form:

$$\chi_{i,\text{syst}}^2 = \frac{1}{1 - \rho_i^2} \left(\frac{(a_{i,1} - a_{0,i})^2}{\sigma_{a_i}^2} + \frac{(a_{i,2} - a_{0,i})^2}{\sigma_{a_i}^2} - \frac{2\rho_i(a_{i,1} - a_{0,i})(a_{i,2} - a_{0,i})}{\sigma_{a_i}^2} \right), \quad (4.8)$$

where we assume the same prior value $a_{0,i}$ and uncertainty σ_{a_i} for both nuisance parameters. For the following of this paper we assume a full correlation ($\rho = 1$) for both, oscillation priors and normalization uncertainties.

In order to define the sensitivity of the experiment to CP violation, we define the test statistics

$$\Delta\chi^2 = \chi_{\delta_{CP}}^2 - \chi_{\text{best}}^2, \quad (4.9)$$

where $\chi_{\delta_{CP}}^2$ is the minimized χ^2 of Eq. 4.1 at a fixed value of δ_{CP} (true or test), while χ_{best}^2 is the minimum χ^2 obtained when δ_{CP} is allowed to vary over the full range of possible values.

The significance to observe CP violation is evaluated by computing $\chi_{\delta_{CP}}^2$ in the two CP conserved cases ($\delta_{CP} = 0$ and $\delta_{CP} = \pi$), and taking the smallest $\Delta\chi^2$:

$$\Delta\chi^2 = \min(\Delta\chi_0^2, \Delta\chi_\pi^2). \quad (4.10)$$

In the following section, the systematics are assumed to be fully correlated between the two baselines but we have checked that the effect on the CPV discovery potential is negligible if we change the degree of correlation.

5 Results

The assumed experimental setup is described in Ref. [5]. Following the incremental approach, an initial 20 kton double phase LAr LEM-TPC (GLACIER [12, 22]) is complemented with a magnetized muon detector (MIND [13, 23]). A second 50 kton detector can be added to reach a total of 70 kton. The sensitivity to measure CP violation in the dual baseline was studied for both detector sizes. In the simulations performed for this paper, the field cage of the 20 kton detector is approximated with a cylinder of radius 33 m and height 20 m, corresponding to an instrumented volume of 17100 m³ and an active mass of 23.9 kton.

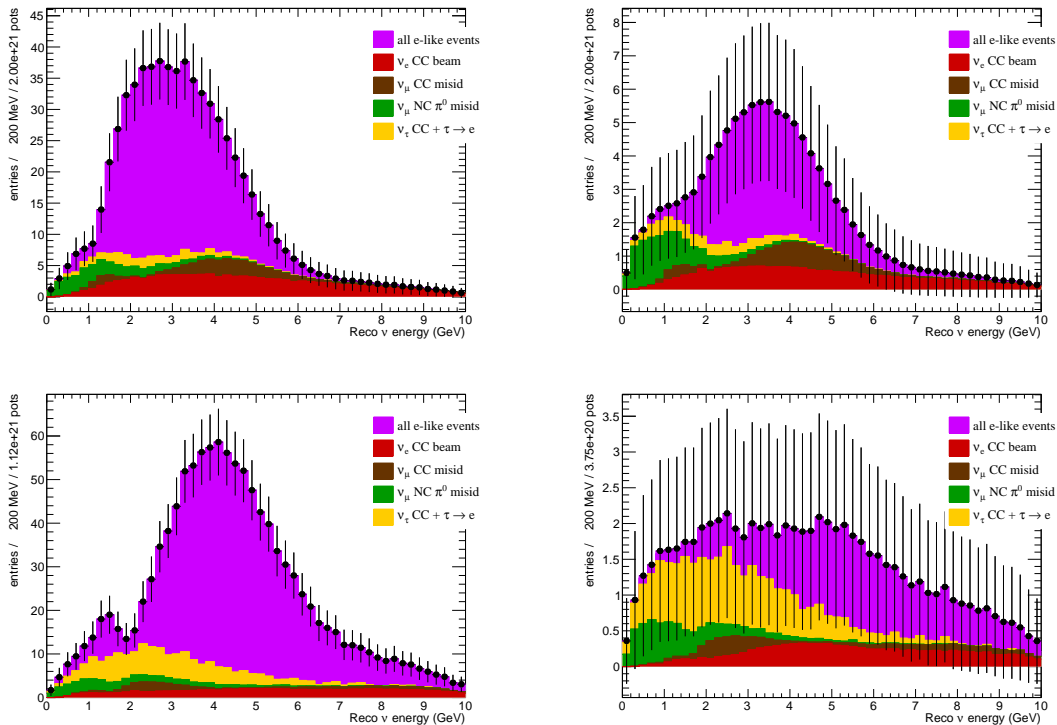


Figure 9. Reconstructed energy spectra for the Protvino-to-Pyhäsalmi (P2P) (top) and the CERN-to-Pyhäsalmi (C2P) (bottom) in positive horn polarity (left) and negative horn polarity (right) for the 20 kton detector. The δ_{CP} is $-\pi/2$ and the hierarchy is normal.

For the P2P beam we assume a total integrated 4×10^{21} POT with a 50% sharing of negative and positive polarity while for the C2P beam we take 1.5×10^{21} POT with a 75-25% sharing between the negative and the positive horn polarity using the SPS GLB optimisation fully described in Ref. [14]. In order to illustrate the expected signal, the spectrum of events in the electron-like sample for $\delta_{CP} = -\pi/2$ for P2P and C2P is shown in Fig. 9: most of the selected events come from oscillated neutrinos while the background is due to NC, intrinsic ν_e and $\nu_\mu \rightarrow \nu_\tau$ oscillated neutrinos.

5.1 CP-violation discovery potential for the dual beam facility

The CPV sensitivity the LBNO configuration is provided by the information contained in the shape of the e-like event distribution for neutrino and antineutrino modes, in particular in the region around the 1st and the 2nd oscillation maxima.

The sensitivity as a function of the true value of the δ_{CP} phase is shown in Fig. 10 for C2P only, P2P only and their combination assuming NH. We see that each baseline separately can reach a 3σ determination of CP-violation ($\Delta\chi^2 > 9$) for $\sim 40\%$ of the values of the δ_{CP} phase. The combination of the two beams, instead, would allow to establish CP-violation at 3σ for $\sim 60\%$ of values of δ_{CP} even with a 20 kton far detector.

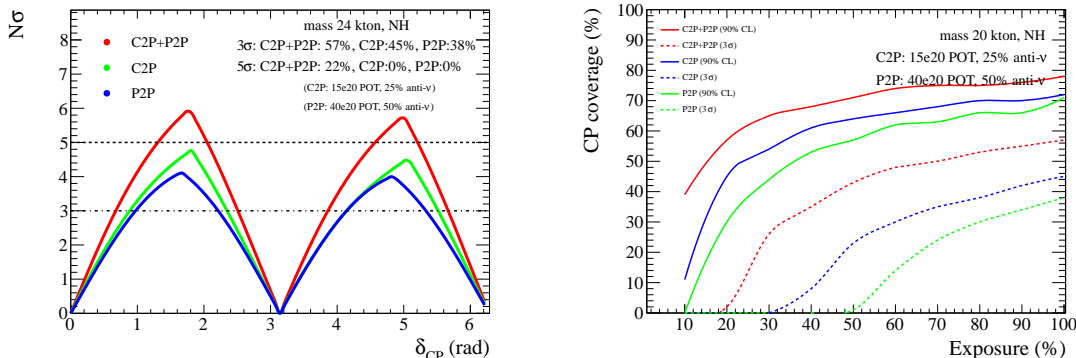


Figure 10. Left: $\sqrt{\Delta\chi^2} = N\sigma$ as a function of the true value of δ_{CP} for CP-violation discovery. Right: Sensitivity to CP-violation in terms of the fraction of δ_{CP} values for which $\delta = 0, \pi$ can be excluded, as a function of the total exposure. Both plots are obtained assuming a 20 kton far detector and NH.

The same sensitivities assuming the same exposure but a larger, 70 kton far detector, are shown in Fig. 11. A larger detector and the combination of the two beams would allow to measure CPV at more than $3(5)\sigma$ for the $70(50)\%$ of the true values of δ_{CP} . Similar results are obtained in the case of inverted hierarchy.

5.2 Advantages of the dual baseline configuration

When considering the combination of two beams, there are a number of effects which lead to better performances. In this section, we will consider separately the following factors which may improve the sensitivity to δ_{CP} :

- a dual beam facility allows for a greater number of events, decreasing the statistical uncertainty;
- combining beams at the same detector may allow for the cancellation of systematic uncertainties;
- both beams have access to different parts of the oscillation parameter space, and the information that they each provide will be complementary, increasing the overall sensitivity.

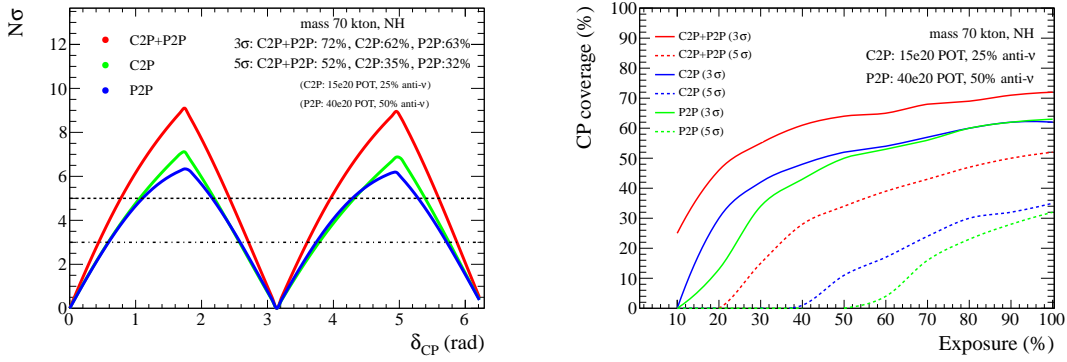


Figure 11. Left: $\sqrt{\Delta\chi^2} = N\sigma$ as a function of the true value of δ_{CP} for CP-violation discovery. Right: Sensitivity to CP-violation in terms of the fraction of δ_{CP} values for which $\delta = 0, \pi$ can be excluded, as a function of the total exposure. Both plots are obtained assuming a 70 kton far detector and NH.

The use of two beams significantly increases the total number of neutrino interactions, without requiring to accumulate POT from a single accelerator complex for which it would be necessary to run the experiment for more years. Adding P2P will help to reduce the statistical uncertainty of the observed rates and allow for an improved sensitivity to δ_{CP} .

The additional sensitivity obtained thanks to the combination of C2P and P2P goes beyond the simple additional statistical power brought by the P2P beam. To establish this, we must compare the combined beams configuration to a single beam facility with an increased exposure, chosen to mitigate any statistical advantage. This can be obtained by scaling the total POT of the C2P beam to add the additional statistical power brought by the P2P beam. In our calculation we assumed a beam power delivered by the Protvino accelerator with a proton beam energy of 70 GeV and a total exposure of 40×10^{20} POT. The equivalent power of the C2P beam, using a proton beam of 400 GeV is then given by:

$$N_{\text{POT}}^{\text{C2P}}_{\text{equiv}} = 40 \times 10^{20} \text{POT} \frac{70}{400} = 7 \times 10^{20} \text{POT}. \quad (5.1)$$

Consequently in the single C2P beam scenario one has to increase the total number of POT to 22×10^{20} POT. To remove the statistical advantage of the dual beams configuration we compare the CPV sensitivity of the scenario with two beams and 15×10^{20} POT for C2P to that of a single beam from CERN with an exposure of 22×10^{20} POT. This is illustrated in Fig. 12. As it is evident from this figure, the sensitivity to CPV is better when operating two beams. To reach a similar sensitivity in the single beam scenario, $\sim 30 \times 10^{20}$ POT should be collected for the C2P beam. This confirms the phenomenological expectation that a dual beam scenario, which combines information from two different baseline distances, will allow an increase in precision unobtainable by an equivalent increase in exposure at a single beam facility.

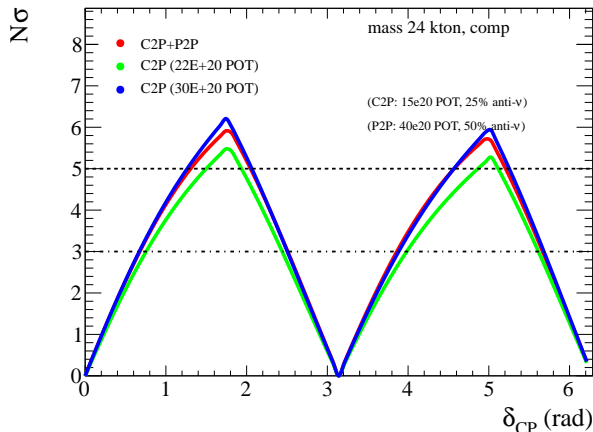


Figure 12. Comparison of the CPV sensitivity obtained with two neutrino beam and a 20 kton far detector to the CPV sensitivity obtained with a single beam and a larger far detector.

6 Conclusions

The proposed LBNO experiment is the outcome of a six year program of feasibility studies supported by the European Commission. The proposed experiment foresees in the phase I a 20 kton underground liquid Argon detector located at the Pyhäsalmi mine, to be incremented to a 70 kton detector in the phase II. A neutrino beam produced at the SPS accelerator at CERN will allow an unambiguous determination of the MH and give a large change to discover CP violation in the leptonic sector.

In this paper we have shown how the physics case can be further enhanced by coupling the neutrino beam from CERN with an additional beam from the Protvino IHEP accelerator complex. The Protvino beam has been optimised to study CP violation and the combination of C2P and P2P will provide a 3σ measurement of δ_{CP} for the 50% of the true values of δ_{CP} in the phase I. With a 70 kton detector, a better sensitivity to CPV will be reached: assuming the two beams with the same exposure a 3σ sensitivity to CP violation can be reached for the 80% of the true values of δ_{CP} phase-space.

In the two beam scenario, we find that the sensitivity improvement goes beyond the simple statistical increase of having more neutrino interactions at the Far Detector since some of the degeneracies of the parameters involved in the neutrino mixing can be resolved by the combination of the two beams at different L/E .

We conclude that an alternative solution to explore MH and CPV in the leptonic sector can be considered with two conventional neutrino beams with modest powers below the 1 MW threshold. Two such beams might be easier to operate than a single multi-MW neutrino beam, which so far has never been achieved. A study of the dependency of the CPV sensitivity on the systematic uncertainties and on the oscillation parameter priors for the dual baseline experiment has been performed and we have shown that in this configuration a discovery level for CPV can be achieved with realistic assumptions on the beam, the detector and the systematic errors.

Acknowledgments

We are grateful to the European Commission for the financial support of the project through the FP7 Design Studies LAGUNA (Project Number 212343) and LAGUNA-LBNO (Project Number 284518). We would also like to acknowledge the financial supports of the Lyon Institute of Origins LabEx program (ANR-10-LABEX-66). In addition, participation of individual researchers and institutions has been further supported by funds from ERC (FP7).

References

- [1] Z. Maki, M. Nakagawa and S. Sakata, “Remarks on the unified model of elementary particles,” *Prog. Theor. Phys.* **28** (1962) 870.
- [2] B. Pontecorvo, “Neutrino Experiments and the Problem of Conservation of Leptonic Charge,” *Sov. Phys. JETP* **26** (1968) 984 [*Zh. Eksp. Teor. Fiz.* **53** (1967) 1717].
- [3] F. P. An *et al.* [DAYA-BAY Collaboration], “Observation of electron-antineutrino disappearance at Daya Bay,” *Phys. Rev. Lett.* **108**, 171803 (2012) [arXiv:1203.1669 [hep-ex]].
- [4] K. Abe *et al.* [T2K Collaboration], “Observation of Electron Neutrino Appearance in a Muon Neutrino Beam,” *Phys. Rev. Lett.* **112** 061802 (2014) [arXiv:1311.4750 [hep-ex]].
- [5] A. Stahl *et al.*, Expression of Interest for a “Very long baseline neutrino oscillation experiment (LBNO).”; CERN SPSC, June, 2012. (CERN-SPSC-2012-021 (SPSC-EOI-007)).
- [6] S. K. Agarwalla *et al.* [LAGUNA-LBNO Collaboration], “The mass-hierarchy and CP-violation discovery reach of the LBNO long-baseline neutrino experiment,” *JHEP* **1405**, 094 (2014) [arXiv:1312.6520 [hep-ph]].
- [7] C. Adams *et al.* [LBNE Collaboration], “The Long-Baseline Neutrino Experiment: Exploring Fundamental Symmetries of the Universe,” arXiv:1307.7335 [hep-ex].
- [8] M. Bass *et al.* [LBNE Collaboration], “Baseline optimization for the measurement of CP violation and mass hierarchy in a long-baseline neutrino oscillation experiment,” arXiv:1311.0212 [hep-ex].
- [9] E. Kearns *et al.* [Hyper-Kamiokande Working Group Collaboration], “Hyper-Kamiokande Physics Opportunities,” arXiv:1309.0184 [hep-ex].
- [10] T. Patzak [LAGUNA-LBNO Collaboration], “LAGUNA and LAGUNA-LBNO: Future megaton neutrino detectors in Europe,” *Nucl. Instrum. Meth. A* **695**, 184 (2012).
- [11] A. Rubbia, “LAGUNA-LBNO: Design of an underground neutrino observatory coupled to long baseline neutrino beams from CERN,” *J. Phys. Conf. Ser.* **408**, 012006 (2013).
- [12] A. Rubbia, “Underground Neutrino Detectors for Particle and Astroparticle Science: The Giant Liquid Argon Charge Imaging Experiment (GLACIER),” *J. Phys. Conf. Ser.* **171** (2009) 012020 [arXiv:0908.1286 [hep-ph]].
- [13] T. Abe *et al.* [ISS Detector Working Group Collaboration], “Detectors and flux instrumentation for future neutrino facilities,” *JINST* **4**, T05001 (2009) [arXiv:0712.4129 [physics.ins-det]].

- [14] S. K. Agarwalla *et al.* [LAGUNA-LBNO Collaboration], “Optimised sensitivity to leptonic CP violation from spectral information: the LBNO case at 2300 km baseline,” arXiv:1412.0593 [hep-ph].
- [15] J. M. Paley [NOvA and LBNE Collaborations], “The search for CP violation and the determination of the neutrino mass hierarchy in NOvA and LBNE,” PoS ICHEP **2012** (2013) 393.
- [16] P. Coloma and E. Fernandez-Martinez, “Optimization of neutrino oscillation facilities for large θ_{13} ,” JHEP **1204** (2012) 089 [arXiv:1110.4583 [hep-ph]].
- [17] J. Arafune, M. Koike and J. Sato, “CP violation and matter effect in long baseline neutrino oscillation experiments,” Phys. Rev. D **56**, 3093 (1997) [Erratum-ibid. D **60**, 119905 (1999)] [hep-ph/9703351].
- [18] V. Barger, D. Marfatia and K. Whisnant, “Breaking eight fold degeneracies in neutrino CP violation, mixing, and mass hierarchy,” Phys. Rev. D **65** (2002) 073023 [hep-ph/0112119].
- [19] L. S. Barabash, S. A. Baranov, Y. A. Batusov, S. A. Bunyatov, V. Y. Valuev, I. A. Golutvin, O. Y. Denisov and M. Y. Kazarinov *et al.*, “The ‘IHEP-JINR Neutrino Detector’ at neutrino beams of the U-70 accelerator,” Instrum. Exp. Tech. **46** (2003) 300 [Prib. Tekh. Eksp. **46** (2003) 20]. DOI: <http://dx.doi.org/10.1023/A:1024406219896>
- [20] OMEGA Project, Nov.prob.fund.fiz. 2(9) 2010; <http://www.ihep.ru/>
- [21] A. Longhin, “Optimization of neutrino beams for underground sites in Europe,” arXiv:1206.4294 [physics.ins-det].
- [22] A. Rubbia, “Experiments for CP violation: A Giant liquid argon scintillation, Cerenkov and charge imaging experiment?,” hep-ph/0402110.
- [23] A. Cervera, A. Laing, J. Martin-Albo and F. J. P. Soler, “Performance of the MIND detector at a Neutrino Factory using realistic muon reconstruction,” Nucl. Instrum. Meth. A **624**, 601 (2010) [arXiv:1004.0358 [hep-ex]].